Reversal Potential of a Wide Ion Channel. Nonuniform Charge Distribution Effects

Victor Levadny[†] and Vicente Aguilella*

Departamento de Ciencias Experimentales, Universidad Jaume I, 12080 Castellón, Spain

Received: April 12, 2001; In Final Form: June 19, 2001

A theory for the reversal potential V_r in a wide, charged ion channel (i.e., with radius comparable to channel length and Debye's length) embedded in a planar membrane is developed. We analyze the influence of a nonuniform channel charge distribution along the channel axis on V_r. The analysis is performed in the framework of the space charge model, which is generalized for axial nonuniform charge distributions. Two kinds of nonhomogeneity are considered: (1) a symmetrical nonhomogeneous distribution when channel charge is uniformly smeared over the inner surface of channel wall, but it does not extend over the whole surface, and (2) an asymmetrical nonhomogeneous distribution corresponding to some part of the total charge uniformly smeared over the channel wall and some other located on one of the channel entrances. For the first distribution it is shown that even a small deviation from a uniform distribution leads to a significant change in the reversal potential. In particular, the experimentally observed nonmonotonic behavior of V_r for the voltage-dependent anion channel from mitochondria (VDAC) as a function of concentration gradient [Zambrowicz, E. B.; Colombini, M.; *Biophys. J.* **1993**, *65*, 1093.] is explained by invoking the axial nonhomogeneity of channel charge. For the second kind of distribution (which resembles that in VDAC closed states) it is shown that the sign and value of the reversal potential depends on the location of the mobile part of the channel charge. Theoretical results are compared with previously reported experimental data for VDAC but they are valid for any charged multiionic channel where the Nernst−Planck formalism can be applied.

Introduction

A variety of intrinsic membrane proteins form aqueous pores in membranes that allow specific solutes and solvent to cross the membrane. Purified from their biological substrate and placed into a lipid membrane they preserve their basic transport features. Ion channel modeling is among the hottest issues of modern biophysics.[1−5] The zero-current potential, or reversal potential, is one of the main parameters that characterize ion channel function.[6] It is a measure of channel selectivity in the presence of a transmembrane ion concentration gradient. The origin of the reversal potential is the following. Since ion movement across the channel is driven both by solution concentration and electric potential gradient, then for any concentration gradient there is a specific value of transmembrane voltage drop that brings the total channel electric current to zero. This value is called the channel reversal potential V_r. This parameter is widely used in the synthetic membrane electrodiffusion field for estimating porous membrane selectivity[7,8] as well as in biological systems.[9,10] In addition, the measurements of channel selectivity on the basis of V_r allow the estimation of channel net fixed charge.[9,10]

To obtain a correct interpretation of reversal potential measurements, it is desirable to have a proper theoretical description of this transport parameter, which may relate V_r with some structural properties of the channel such as fixed charge, size, dielectric constant, etc. There is considerable literature dealing with theoretical models for ion transport in macroscopic charged pores. The *charged cylindrical model*, also known as *space charge model* (SCM), developed by Osterle and coworkers,[11−15] is one of them. It uses Poisson−Boltzmann's equation for the electrostatics of pore solution and Nernst−Planck and Navier−Stokes equations for ion and solvent transport across the pore. The SCM predicts the transport characteristics of a lot of porous synthetic membranes rather well,[14] but its direct application (as happens with other theoretical models) to aqueous pores produced by proteins in biological membranes faces several problems. For instance, it cannot explain the nonmonotonic reversal potential dependence on ion concentration gradient obtained for some biological channels.[10]

The classical SCM implies two main simplifying assumptions: First, all fixed charges are considered located on the surface of the channel wall, which is assumed cylindrical. Second, channel charges are uniformly smeared over the whole inner wall of the channel. The effects connected with the failure of the first assumption, i.e., charges are distributed within some volume adjoining to the pore wall, were already considered.[16,17] Here we modify the classical SCM so as to account for the effects arising from a nonhomogeneous distribution of channel charge in the axial direction.

There is a great variety of possible nonhomogeneous charge distributions. The aim of the present paper is to demonstrate the importance of taking into account a nonhomogeneous distribution of channel charge for a correct interpretation of reversal potential measurements. To this purpose we consider here two important specific kinds of nonhomogeneity: (1) a symmetrical nonhomogeneous distribution, when the total channel charge is uniformly smeared over some part of the inner surface of channel wall (but not over the whole wall as in the classical SCM) and (2) an asymmetrical nonhomogeneous distribution when one part of the channel charge is uniformly smeared over the channel wall and other one is located at a

* Corresponding author. Tel.: +34−964−728045. Fax: +34-964-728066. E-mail: aguilell@uji.es.

[†] Permanent address: The Scientific Council for Cybernetics, Russian Academy of Sciences; Vavilov str. 34, 333117 Moscow, Russia. E-mail: levadny@guest.uji.es.

10.1021/jp011379u CCC: $20.00
Published on Web 09/15/2001

channel entrance. We will show that for the first kind of nonhomogeneity the behavior of V_r deviates significantly from that predicted by the classical SCM.

Apart from their general theoretical interest, these two kinds of nonhomogeneous distribution resemble the charge distribution of a small protein (30 kDa) that forms aqueous pores in cell membranes: the voltage-dependent anion channel (VDAC) of the mitochondrial outer membrane. This channel can be modeled as a charged cylindrical pore, and it is relatively large (3 nm in diameter and 5 nm long, with a slightly greater effective length[18,19]) compared to other ion channels. Purified from mitochondria and placed into a phospholipid membrane, it exhibits two main conductive levels (connected through the gating process): a high conductance state (called "open state"), for zero or very low transmembrane voltages, and low conductance states (known as "closed states") achieved either at positive or negative applied transmembrane voltages.[20] Some charged residues line the inner wall of the channel, and it is this charge what determines channel selectivity. VDAC is anion selective in the open state (so it has net positive charge in this state), and it is cation selective in the closed states (what implies net negative charge). The exact channel charge distribution is not known, but a great deal of evidence indicates that some charged regions of the channel (denoted by "channel mobile charge") move across the membrane during the gating process [21] causing the channel to switch from anion selectivity to cation selectivity. Therefore, the experimental evidence can be summarized as follows. The total VDAC charge consists of two parts: a negative charge located always inside the channel and a positive charge located inside the channel in the open state and outside the channel in the closed states.

We are aware of only two studies on ion transport across *wide* biological pores as VDAC whose structure has not been determined yet at high enough resolution. Peng et al.[9]—attempting to model ion transport across VDAC channel—divided the aqueous pore volume into two portions each one with its own reversal potential: a charged shell, whose thickness was one Debye's length, with ion-conducting properties as described by Teorell's theory,[22] and a central neutral cylinder of fluid that acted as a shunt. Zambrowicz and Colombini[10] modified this approach in order to explain the dependence of reversal potential on ion concentration gradient for VDAC. In particular, they assumed that the reversal potential is the weighed average of reversal potential across the charged shell and the reversal potential through the central neutral cylinder. However, only harmonic averaging seemed to work properly. Such dependence of the theoretical predictions on the averaging method used for the thickness of the charged shell led these authors to suggest that their theoretical treatment needed further refinement.

One could think that by using a more accurate description of the electric double layer inside the channel—avoiding the sharp partition of the channel interior into two compartments—as that provided by the classical SCM results would agree better with experiments, but the fact is that the SCM fails to explain the nonmonotonic reversal potential dependence on ion concentration gradient.

After considering the basic statements of the SCM we found that the assumption of an axial uniform description of channel charge is the main cause that prevents the SCM from representing biological channels behavior properly. Taking into account that the classical SCM assumes that pore length is much greater than Debye's length, it is not surprising that it is far from being a good model for a short biological ion channel, where usually

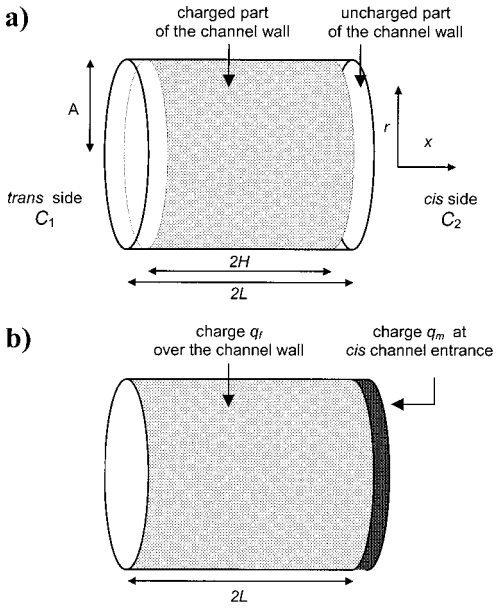

Figure 1. Sketch of the model system representing the channel. The channel trans-entrance corresponds to $x = -L$; the cis-entrance corresponds to $x = L$. (a) Symmetrical nonuniform charge distribution. (b) Asymmetric charge distribution with mobile charge at cis-entrance. Light shadow region represents the channel fixed charge and the dark shadow one represents the channel mobile charge.

pore length and Debye's length are of the same order of magnitude. In fact this assumption means neglecting axial nonhomogeneity, in particular, any end effects.

Here we are comparing our theoretical results with experimental data for VDAC from literature, because the analysis of reversal potential measurements in VDAC channel was the initial motive of our study. But the results obtained here are valid for any multiionic channel in which fixed charge is not homogeneously distributed. A lot of channels as gap junctions and porins fall into this category and could be also the object of this study. As it is known, the electrostatic interaction between mobile ions from solution and fixed channel charges is the leading one in multiionic ion channels. For that reason, we will not consider here any specific interaction between ions and channel nor any effect related to the dielectric constant of the protein.[9]

Description of Model and Discussion

Basic Statements. A charged ion channel embedded in a neutral lipid membrane is considered. It is represented as a pore, cylindrical in shape, with radius A, length $2L$, and with its total net charge being q elementary charges. The membrane separates two electrolyte solutions with different concentrations C_1 and C_2 . The high-concentrated (C_2) solution is denoted as cis-solution, and the low-concentrated (C_1) one is called trans-solution. The cylindrical coordinates x and r with their origin at the center of the pore are used (Figure 1). The membrane itself is impermeable to ions, so that all ion flux takes place across the pore due to diffusion ($C_2 > C_1$) and migration. There is a double electrical layer (DEL) within the pore due to fixed charge q, which influences the ion flux.

In the steady state the electric potential φ in any point inside the channel is the sum of the DEL potential $\psi(x,r)$ and some additional potential $V(x)$. All electric potentials are dimensionless, given in kT/e units. The electric potential difference $V(+L) - V(-L)$ arises in the case of $C_1 \neq C_2$ to ensure net space charge conservation condition in the steady state. This potential drop

across the channel can be measured and it is known as the reversal potential V_r. Theoretically, the reversal potential V_r can be obtained on the basis of the Nernst−Planck equation as the zero-current applied potential. The present development could be applied for any electric potential by using numerical calculations, but we consider here small potentials, $\psi \ll 1$, since such small potentials allow us to obtain a relatively simple analytical expression (See eq A11 in Appendix A).

$$V_r = (1 - \omega^2)\int_{C_1}^{C_2}\langle\psi\rangle \, d \ln C + \omega \ln\left(\frac{C_1}{C_2}\right) \qquad (1)$$

where $\langle\psi\rangle$ is the DEL potential averaged by radius (see eq A7 in Appendix A); $\omega \equiv (D_+ - D_-)/(D_+ + D_-)$ and D_+ and D_- are cation and anion bulk diffusion coefficients, respectively.

In view of this expression 1, the problem of reversal potential calculation is reduced to a correct determination of the DEL potential profile $\psi(x,r)$ inside the channel. The classical SCM assumes that the channel charge q is uniformly smeared over the whole inner wall of the channel, so that the charge space distribution $Q(x,r)$ for $-L \le x \le L$ is

$$Q(x,r) = \frac{q}{2\pi A 2L}\delta(r - A) \qquad (2)$$

and it leads to

$$\langle\psi\rangle = \frac{bq}{C(x)} \qquad (3)$$

where $C(x)$ is the electrolyte concentration at position x of the channel axis and b is a constant determined by channel size (A and L); for a 1:1 electrolyte solution, $b = 1.32 \times 10^{-25}$ mol/A^2L. Equation 3 comes from the common solution of Poisson−Boltzmann equation in cylindrical coordinates (see, e.g., refs 14 and 23). By inserting eq 3 into eq 1, one obtains the classical expression for the reversal potential V_r within the framework of the SCM (A similar result is also obtained from Teorell's approach[15]):

$$V_r = bq(1 - \omega^2)\left(\frac{1}{C_1} - \frac{1}{C_2}\right) + \omega \ln\left(\frac{C_1}{C_2}\right) \qquad (4)$$

Note that eq 1 can be rewritten according to the classical treatment of reversal potential, i.e., as a sum of two contributions: diffusion potential,

$$\phi_{diff} = \omega\left[\ln\left(\frac{C_1}{C_2}\right) - \omega\int_{C_1}^{C_2}\langle\psi\rangle \, d \ln C\right] \approx \omega \ln\left(\frac{C_1}{C_2}\right) \qquad (5)$$

and two Donnan potentials π^{tr} and π^{cis} on both sides of the channel,

$$\pi = \pi^{tr} + \pi^{cis} = \int_{C_1}^{C_2}\langle\psi\rangle d \ln C \qquad (6)$$

For the sake of simplicity—without loss of generality—we will consider only the case $\omega \approx 0$ ($\phi_{diff} = 0$), i.e., similar cation and anion mobilities, as it is in KCl solution where $\omega = -0.02 \approx 0$. In this case $V_r = \pi$. The generalization for $\phi_{diff} \neq 0$ is straightforward.

A Symmetrical Nonuniform Channel Charge Distribution. The approach based on expression 4 is common in the description of ion electrodiffusion across porous synthetic membranes. But its direct application to biological pores (and generally for any small pore whose dimensions are comparable with Debye length) faces problems. In particular, it cannot explain the nonmonotonic reversal potential dependence on ion concentration gradient observed in VDAC channel.[10] Here we will show that the SCM approach can be successfully applied to wide ion channels provided an adequate representation of their charge distributions is given. But instead of the classical expression 4, valid only for a uniform charge distribution, it is necessary to use the general eq 1. Our idea is the following. We think that the first step to generalize the SCM is to account for a nonhomogeneous charge distribution. The simplest way to make this generalization is starting from a simplified model of charge distribution in which the total charge q is smeared uniformly over some fraction H/L of the channel wall (but not over the whole wall as assumed in the SCM). Formally this kind of distribution can be represented as

$$Q(x,r) = \frac{q}{2\pi A \, 2H}\delta(r - A)\,\theta\,(H - |x|) \qquad (7)$$

where $\theta(x)$ is the Heaviside step function. Note that this distribution becomes the classical expression 2 for $H = L$. Mathematically, H/L is the charged fraction of the channel length (Figure 1a). But it is worth to underline that it has a more general meaning. Actually $(L - H)$ describes the effective separation distance between the channel charged zone and the bulk of solution. Therefore, assuming that the charge distribution is given by eq 7 is a possible way of accounting for end effects. Note also that the limit case $H \to 0$ corresponds to a barrier treatment of the charged channel.

The electric potential axial profile $\langle\psi\rangle$ inside the channel following from eq 7 can be represented as (see Appendix B and Figure 2a):

$$\text{for } -L < x < -H \qquad \langle\psi\rangle = \frac{bq}{2C(-H)}\exp[\kappa_{tr}(x + H)] \qquad (8a)$$

$$\text{for } -H < x < H \qquad \langle\psi\rangle = \frac{bq}{2C(x)}\{2 - \exp[-\kappa_{tr}(x + H)] - \exp[\kappa_{cis}(x - H)]\} \qquad (8b)$$

$$\text{for } H < x < L \qquad \langle\psi\rangle = \frac{bq}{2C(H)}\exp[-\kappa_{cis}(x - H)] \qquad (8c)$$

where κ_{tr} and κ_{cis} are the inverse Debye lengths of solutions inside the channel adjacent to the trans and cis entrances, respectively. Note that for the comparison with experimental data one should take into account that eq 8 properly describes the electric potential profile for $\kappa_{tr}H \gg 1$ and that for $\kappa_{cis}H \gg 1$. In contrast to the classical SCM, here the integral in eq 1 needs to be calculated numerically. Figure 3 shows the change of reversal potential with ion concentration gradient $V_r(C_2/C_1)$ calculated from eqs 1 and 8 for different values of H/L. Two limit cases (the classical uniform distribution of charge ($H = L$) and the charge on a single barrier ($H \to 0$)) are shown by thick lines. As Figure 3 shows, the change of reversal potential with concentration ratio is monotonic for a homogeneous charge distribution, while it is not for a nonhomogeneous one. One can see that even a relatively small deviation of H/L from 1 results in a significant change of V_r with respect to the classical treatment prediction from eq 4. In particular, this figure demonstrates a biphasic behavior of $V_r(C_2/C_1)$, i.e., when C_2 is made higher while holding C_1 constant, the reversal potential

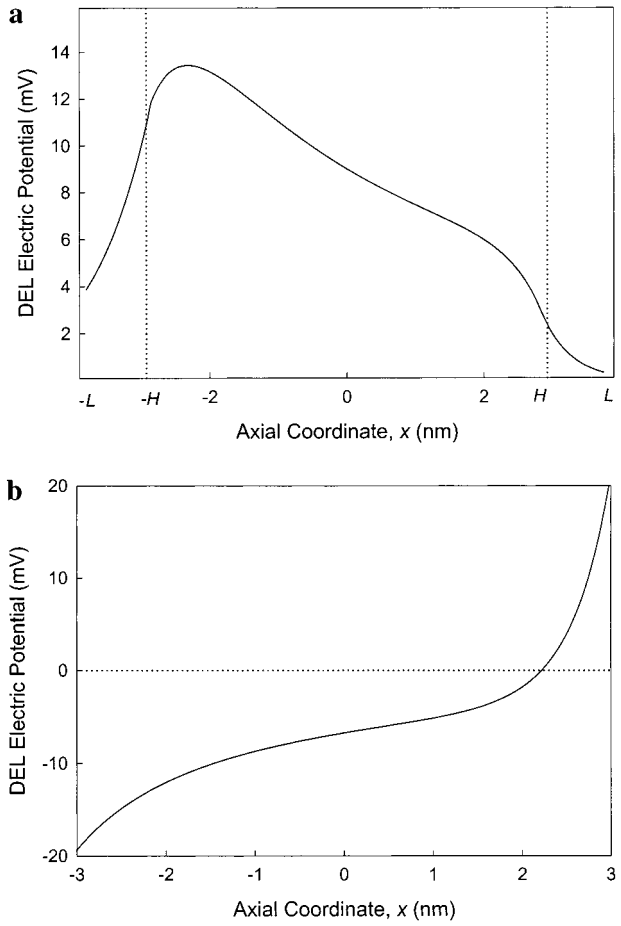

Figure 2. a) The double electric layer potential profile inside channel $\langle\psi\rangle$ for the symmetrical nonuniform charge distribution for $H = 0.75L$. $C_1 = 0.06$ M, $C_2 = 0.6$ M, $q = +3.2$, $A = 1.5$ nm, $2L = 7.5$ nm. (b) The same profile for the asymmetric charge distribution. $q_f = -3$ and $q_m = +6$.

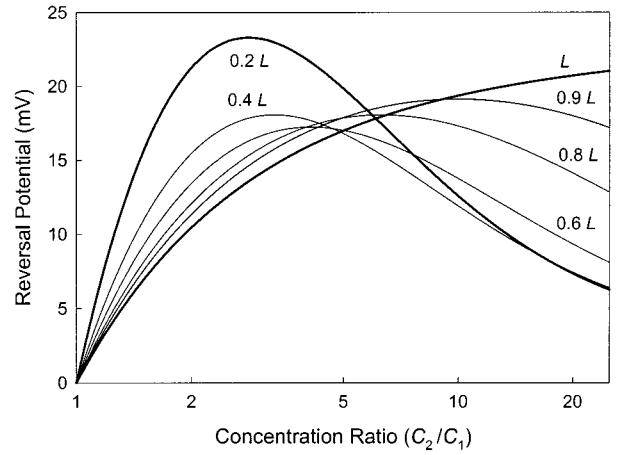

Figure 3. Change of channel reversal potential with ion concentration ratio (C_2/C_1) between both sides of the membrane (for $\omega = 0$) for a non homogeneous symmetrical charge distribution, for different lengths of the charged region $2H$, calculated from eqs 1 and 8. The following parameters were used: the total channel charge was assumed positive $q = +3.2$, the concentration of trans-solution is assigned a fixed value $C_1 = 0.06$ M, and the concentration of cis-solution is varied. The channel length is $2L = 7.5$ nm,[18] and the channel radius $A = 1.5$ nm as used by Zambrowicz and Colombini.[10]

increases at the onset, reaches a maximum and then decreases. To clarify the physical meaning of such biphasic behavior let us estimate the integral in eq 1 for the case here considered.

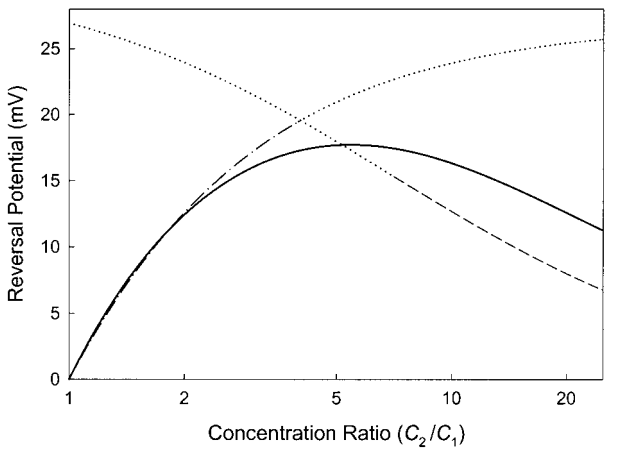

Figure 4. Explanation of the biphasic behavior of VDAC channel reversal potential $V_r(C_2/C_1)$ (solid line) shown in Figure 3. The dash−dot line represents V_r values in the limiting case of small concentration gradients. The dash line represents the V_r values in the region of large concentration gradients (see main text). Dot lines show the calculations of those two limiting cases in the region where they are not valid.

Assuming that $\Delta \equiv 1 - H/L \ll 1$ is a small parameter, one obtains from eqs 1 and 8 the following approximate estimation of reversal potential V_r:

$$V_r = \langle\psi\rangle_{x=H} - \langle\psi\rangle_{x=-H} + o(\Delta^2) \approx \pi^{tr} + \pi^{cis} = bq\left[\left(\frac{1}{C_1} - \frac{1}{C_2}\right) - \frac{\Delta}{2}\frac{C_2}{C_1^2}\right] \quad (9)$$

As it follows from eq 9, the dependence $V_r(C_2/C_1)$ is determined by two main processes: the decrease of cis-side Donnan potential $\pi^{cis} = \langle\psi\rangle_{x=H} = bq/C(H)$; and the decrease of trans-side Donnan potential $\pi^{tr} = \langle\psi\rangle_{x=-H} = bq/C(-H)$. The first process dominates for small concentration gradients, and the second one dominates in the case of great concentration gradients. Actually for a small concentration difference, ($C_2 \sim C_1$), one obtains from eq 9

$$V_r \approx bq\left(\frac{1}{C_1} - \frac{1}{C_2}\right) = \text{const} - \pi^{cis} \approx \text{const} - \frac{bq}{C_2} \quad (10)$$

and the first process prevails. Therefore, the reversal potential increases with C_2 (see dot line in Figure 4). For high concentration gradients, $C_2 \gg C(1/2 - H/2L)^{1/2}$, eq 9 becomes

$$V_r \approx \frac{bq}{C_1}\left(1 - \frac{\Delta C_2}{2C_1}\right) \approx \pi^{tr} = \text{const} - \left(\frac{bq\Delta}{2C_1^2}\right)C_2 \quad (11)$$

where it is seen that the second process dominates. V_r decreases as C_2 increases (see dashed line in Figure 4). The comparison of our theoretical calculations, based on eqs 1 and 8, with experimental results for VDAC channel[10] is shown in Figure 5. One can see a remarkable agreement with experiment. For the theoretical calculation the net VDAC charge was assumed to be $+3.2e$. This value is in a good agreement with earlier reported indirect estimations ($+3.5e$ for *N. Crassa* VDAC[10] and $+2.5e$ for *S. Cerevisiae* VDAC[9]). The length of the charged region H was assumed to be $0.75L$. The fact that such a small deviation (25%) from channel charge homogeneity leads to a good agreement with the experimental results means that the biphasic behavior of VDAC reversal potential can be explained in terms of end effects of electric potential profile inside the

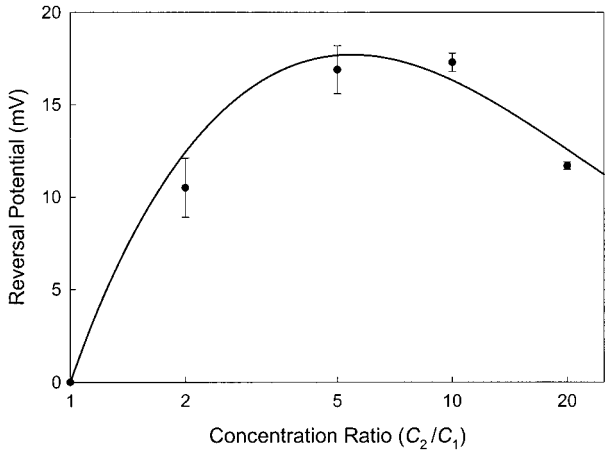

Figure 5. Comparison of V_r calculations, according to eqs 1 and 8, with experimental data reported for *N. crassa* VDAC in KCl from ref 10. The net channel charge assumed for calculations is $q = +3.2$; the concentration of trans-solution is $C_1 = 0.06$ M, the effective channel length is $2L = 7.5$ nm,[18] the channel radius is $A = 1.5$ nm, and the length of the charged region is $H = 0.83L$.

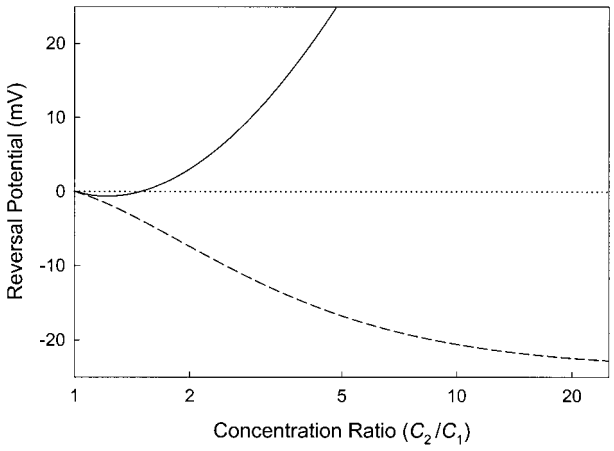

Figure 6. Predicted change of channel reversal potential with KCl concentration ratio between both sides of the membrane (C_2/C_1) for an asymmetrical fixed charge distribution in the case of $q_f = -2.5$ and $q_m = +5$ (see explanation in the text). Dashed line corresponds to the cis-closed state of the channel and solid line corresponds to the trans-closed state.

channel. In other words, $(L - H)$ can be regarded as the effective separation distance between the bulk of solution and the channel entrance. As for the above-mentioned condition of $\kappa H \gg 1$, it is satisfied here. Note that the minimum concentration in Zambrowicz and Colombini's experiments was 0.06 M, which leads to $\kappa H \geq 2.3$ in the whole range of concentration explored.

An Asymmetrical Charge Distribution. To demonstrate the importance of nonhomogeneous charge distributions for biological channels, we consider here also another kind of distribution associated with the closed state of VDAC channel. As we mentioned in the Introduction, the total VDAC charge consists of two parts: the negative charge $q_f < 0$ located always inside the channel (also denoted here as "fixed" charge), and the positive charge (also denoted here as "mobile" charge) $q_m > 0$, located inside the channel in the open state and outside the channel in the closed states. Moreover, in closed states the mobile charge q_m can be either in trans-solution (trans-closed state) or in cis-solution (cis-closed state).[20]

Therefore, let us assume that the fixed charge q_f is uniformly smeared over the whole inner channel wall, and the mobile charge q_m is located at one of the channel entrances and smeared over the channel cross section. For example, if q_m is located at the cis-entrance (Figure 1b), this kind of distribution can be mathematically represented as

$$Q(x, r) = \frac{q_f}{2\pi A\, 2L}\delta(r - A) + \frac{q_m}{\pi A^2}\delta(x - L) \qquad (12)$$

Note the difference between eq 12 and eq 2. The electric field created by fixed charge q_f is described as before by eq 3. As for the mobile charge q_m, the calculation of its electric field is not straightforward. In addition, there is not enough information about the specific channel entrance structure. Therefore, this electric field due to q_m needs to be represented by means of some reasonable model. Here we make use of a Gouy−Chapman-like expression for the potential profile inside the channel owing to q_m. It allows us to represent the total electric potential profile $\langle\psi\rangle$ inside channel for the cis-closed state as follows (see also Figure 2b):

$$\langle\psi\rangle = b\frac{q_f}{C(x)} + \psi_0 \exp[\kappa_{cis}(x - L)] \qquad (13)$$

where ψ_0 is the potential created by q_m just in cis -entrance:

$$\psi_0 = \frac{e^2}{\epsilon kT}\frac{q_m}{\pi A^2 \kappa_{cis}} \qquad (14)$$

The solid line in Figure 6 shows the dependence $V_r(C_2/C_1)$ calculated from eq 1 and eqs 13 and 14 for $q_f < 0$ and $q_m > 0$ and $|q_m| \approx 2|q_f|$ (cis-closed VDAC state). A similar calculation for the mobile charge location at the other channel entrance is also shown by the dashed line. It is seen that the absolute value of V_r increases almost monotonically for both cases (except for very low concentration gradients in the case of cis-closed state), but the sign of the reversal potential in the trans-closed state (V_r^{tr}) is positive and it is negative in the cis-closed state (V_r^{cis}). To clarify the physical origin of such behavior let us estimate the integral in eq 1 for these cases. By taking into account that $C_2 > C_1$ and $\omega = 0$, then eqs 1 and 13 (and the analogous equations in the trans-closed state) lead to

$$V_r^{tr} = bq_f\left(\frac{1}{C_1} - \frac{1}{C_2}\right) + \frac{aq_m}{\sqrt{C_1}}\ln\left(\frac{C_2}{C_1}\right) \approx \frac{aq_m}{\sqrt{C_1}}\ln\left(\frac{C_2}{C_1}\right) \qquad (15a)$$

$$V_r^{cis} = bq_f\left(\frac{1}{C_1} - \frac{1}{C_2}\right) + \frac{aq_m}{\sqrt{C_2}}\ln\left(\frac{C_2}{C_1}\right) \approx \frac{bq_f}{C_1} \qquad (15b)$$

where $a \equiv (4\pi^2A^4\epsilon kT)^{-1/2}$. Equation 15a shows that the reversal potential in the trans-closed state is mainly determined by q_m itself and by the ion concentration gradient. But in the cis-closed state mainly q_f determines it . The mobile charge is screened by cis-solution in this case and its contribution to the total electric field inside the channel decreases as C_2 increases.

Note that eq 12 assumes that the mobile charge q_m is just at the channel entrance. Should mobile charge be located near channel entrances, then the difference between reversal potential in different closed states shown on Figure 6 would not be so pronounced. This question waits for experimental studies.

Conclusions

The behavior of the reversal potential V_r of a wide, charged ion channel embedded in a planar membrane upon variation of concentration gradient in the bathing solutions has been

considered theoretically. We have analyzed the influence of the channel charge axial nonhomogeneity on V_r. Two kinds of nonhomogeneity were considered: a symmetrical nonhomogeneous distribution when channel charge q is uniformly smeared over some fraction of the inner surface of channel wall, and an asymmetrical nonhomogeneous distribution in which one part of the charge is uniformly smeared over the channel wall and other part is located at the channel entrance. The analysis has been done in the framework of the space charge model, which was generalized for an axial nonhomogeneous charge distribution. As for the first kind of nonhomogeneity, we have determined that even a small deviation from the uniform charge distribution leads to a significant change in reversal potential behavior. In particular, we have shown that the decrease of V_r in VDAC observed experimentally for large concentration gradients[10] can be explained by invoking axial nonhomogeneity of channel charge distribution.

For the second kind of nonhomogeneity it was shown that the sign and value of the reversal potential depends on the mobile charge location. As an example we have considered the case when mobile charge has opposite sign than the fixed charge (the case of VDAC). It turns out that the reversal potential is determined mainly by the mobile part of the channel charge if this is located in the low concentration entrance. However, if it is located in the high concentration entrance, then the reversal potential is determined by the fixed part of the channel charge.

We have compared our theoretical results with experimental data for VDAC from literature.[10] However, our treatment is valid not only for this specific channel, but for any charged, multiionic channel where the Nernst−Planck formalism can be applied.

Acknowledgment. V.L. thanks financial support from Generalitat Valenciana and Universitat Jaume I through a grant for invited scientists. V.A. thanks financial support from Fundació Caixa-Castelló (Project P1B98-12) and from DGICYT (Project PB98-0419).

Appendix A

The basic equations of the space charge model (SCM) are Nernst−Planck's, Poisson's, and Boltzmann's along with the charge conservation equation at the steady state (neglecting viscosity)

$$\vec{J}_i = -D_i(\vec{\nabla}C_i + Z_iC_i\vec{\nabla}\varphi) \tag{A1}$$

$$\nabla^2\varphi = -\frac{e^2}{\epsilon kT}\sum\gamma_iZ_iC_i \tag{A2}$$

$$\vec{\nabla}\cdot\vec{J}_i = 0 \tag{A3}$$

$$C_i(x,r) = C(x)\exp[-Z_i\varphi(x,r)] \tag{A4}$$

where $\vec{J}_i$ is the flux density of the ith ion, and D_i, Z_i, and γ_i are its diffusion coefficient, valence, and its fraction in solution, respectively; e is the elementary charge, ϵ is the solution dielectric permittivity; φ is the electric potential (all potentials are dimensionless, i.e., in kT/e units); $C(x)$ is the axial concentration profile inside channel, which is assumed linear along the x direction, $C(x) = 0.5[(C_2 - C_1)x/L + C_1 + C_2]$; and $C_i(x,r)$ is the concentration of the ith ion at the point (x,r).

The total electric potential φ in any point of the channel under steady-state conditions is the sum of the DEL potential ψ (which is a function of x and r) and some additional potential V (which is a function of x only):

$$\varphi(x, r) = \psi(x, r) + V(x) \tag{A5}$$

The electric potential $V(x)$ arises inside channel to ensure the charge conservation condition (A3) in the steady state. From eqs A1−A5 the density of electric current I across the channel, for a binary electrolyte, can be defined as

$$I = e\langle Z_+(J_+)_x + Z_-(J_-)_x\rangle = L_{11}\frac{dV}{dx} + L_{12}\frac{d\ln C}{dx} \tag{A6}$$

where $(J_\pm)_x$ denotes the x-component of the vector $\vec{J}_\pm$; "$\langle\ \rangle$" denotes the average over the radial coordinate, i.e.,

$$\langle f\rangle = \frac{2}{A^2}\int_0^A f(r)r\,dr \tag{A7}$$

and Onsager coefficients L_{11} and L_{12}, which can be obtained from eqs A1−A5, are (for a 1:1 electrolyte):

$$L_{11} = -\frac{2C}{A^2}\int_0^A[D_-e^{\psi} + D_+e^{-\psi}]r\,dr = \frac{2C}{A^2}(D_- + D_+)\int_0^A(\omega\psi - 1)r\,dr + o(\psi^2) \approx C(D_- + D_+)(\omega\langle\psi\rangle - 1) \tag{A8}$$

$$L_{12} = \frac{2C}{A^2}\int_0^A[D_-e^{\psi} - D_+e^{-\psi}]rdr = \frac{2C}{A^2}(D_- + D_+)\int_0^A(\psi - \omega)rdr + o(\psi^2) \approx C(D_- + D_+)(\langle\psi\rangle - \omega) \tag{A9}$$

where $\omega \equiv (D_+ - D_-)/(D_+ + D_-)$. The first-order approximation of L_{11} and L_{12} in eqs A8 and A9 corresponds to $\langle\psi\rangle \ll 1$. To obtain higher order approximations, a numerical solution is needed. Equations A1−A9 are the common treatment of ion transport within the framework of the SCM without viscosity terms (see, e.g., ref 14 and references therein). The small length of ion channels allows us to neglect here the solution viscosity.

The additional electric potential profile $V(x)$ follows from eq A6 as zero-current profile

$$V(x) = -\int_{-L}^{x}\frac{L_{12}(x)}{L_{11}(x)}\frac{d\ln C}{dx}dx = -\int_{C_1}^{C(x)}\frac{L_{12}}{L_{11}}d\ln C \tag{A10}$$

The total drop of this potential across the channel can be measured and it is known as the reversal potential, V_r, i.e., $V_r = V(L)$ when assuming that $V(-L) = 0$. For small potentials, $\langle\psi\rangle \ll 1$, it becomes

$$V(x) = \int_{C_1}^{C(x)}\frac{\langle\psi\rangle - \omega}{1 - \langle\psi\rangle\omega}d\ln C \approx (1 - \omega^2)\int_{C_1}^{C(x)}\langle\psi\rangle d\ln C + \omega\ln\frac{C_1}{C(x)} \tag{A11}$$

Two additional comments follow: first, for a uniform charge distribution, by inserting eq 3 from the main text into eqs A5,

A7−A9, and A11, one can obtain the following steady-state electric potential $\langle\varphi\rangle$:

$$\langle\varphi\rangle = \frac{bq}{C_1} + \omega\left\{\ln\frac{C_1}{C(x)} - bq\omega\left[\frac{1}{C_1} - \frac{1}{C(x)}\right]\right\} = \frac{bq}{C_1} + \phi_{\text{diff}} \tag{A12}$$

Therefore, for $\omega = 0$ (i.e., when $D_+ = D_-$ and $\phi_{\text{diff}} = 0$) the steady-state electric potential profile inside the channel is the same as in the absence of ion concentration gradient (i.e., when $C_1 = C_2$) for any concentration gradient. A similar statement can be proved for nonuniform charge distributions too. Second, it is worth comparing this result from the SCM with that from Teorell's theory:[10,22]

$$V_r = \ln\frac{R_2}{R_1} + \omega\ln\left[\frac{C_1(R_1D_+ + D\_/R_1)}{C_2(R_2D_+ + D\_/R_2)}\right] \tag{A13}$$

where R_i is the Donnan ratio, $R_i = [1 + (X/2C_i)^2]^{1/2} - X/2C_i \approx 1 - X/2C_i$, and X is the effective concentration of channel space charge. One can easily obtain that eq A13 transforms into eq A11 and vice versa if $X = 2b$. Hence, the SCM corresponds to the modified Teorell's theory for large channels—coined as LCT by Zambrowicz and Colombini[10]—when the charged cylindrical shell fills the entire VDAC pore.

Appendix B

The DEL potential profile $\psi(x,r)$ inside the channel is commonly described by Poisson−Boltzmann's equation, which is written in cylindrical coordinates for $|\psi| \ll 1$ as

$$\frac{\partial^2\psi}{\partial r^2} + \frac{1}{r}\frac{\partial\psi}{\partial r} + \frac{\partial^2\psi}{\partial x^2} - \kappa^2\psi = 0 \tag{B1}$$

where κ is the inverse Debye length of the solution of concentration C inside the channel, $\kappa^2 = 2e^2N_AC/kT\epsilon$ (for 1:1 electrolyte); k is Boltzmann's constant; and N_A is Avogadro's number. In the classical SCM, the term $\partial^2\psi/\partial x^2$ is neglected by assuming that $A/L \ll 1$, but actually it means neglecting any axial nonhomogeneity. We bypass this mathematical problem by taking into account that we need only the averaged value of $\psi(x,r)$ over the radial coordinate. Multiplying (B1) by $r\mathrm{d}r$ and integrating it in accordance with eq A7 and taking into account that

$$\int_0^A r\frac{\partial^2\psi}{\partial r^2}\mathrm{d}r = -\int_0^A \frac{\partial\psi}{\partial r}\mathrm{d}r + A\frac{\partial\psi(r=A)}{\partial r} = -\int_0^A \frac{\partial\psi}{\partial r}\mathrm{d}r + A\frac{\sigma}{\epsilon} \tag{B2}$$

where σ is the surface charge density, one obtains from eq B1 the following equation for the averaged potential $\langle\psi\rangle$, defined according to eq A7,

$$\frac{\mathrm{d}^2\langle\psi\rangle}{\mathrm{d}x^2} - \kappa^2\langle\psi\rangle = \frac{2\sigma}{A\epsilon} \tag{B3}$$

To obtain the DEL potential profile from eq B3, it has to be combined with the boundary conditions $\langle\psi\rangle_{x=-\infty} = \langle\psi\rangle_{x=+\infty} = 0$ and the common matching conditions for any points where σ has a discontinuity. In the first case of charge nonhomogeneity studied here, we assume that the potential profile at the channel midpoint is determined by eq 3 (see main text) to ensure the solution transformation to the common SCM solution for a uniform charge distribution.

References and Notes

(1) Levitt, D. G. *J. Gen. Physiol.* **1999**, *113*, 789.
(2) Nonner, W.; Chen, D. P.; Eisenberg, B. *J. Gen. Physiol.* **1999**, *113*, 773.
(3) Moy, G.; Corry, B.; Kuyucak, S.; Chung, S.-H. *Biophys. J.* **2000**, *78*, 2349.
(4) Corry, B.; Kuyucak, S.; Chung, S.-H. *Biophys. J.* **2000**, *78*, 2364.
(5) Cardenas, A. E.; Coalson, R. D.; Kurnikova, M. G. *Biophys. J:* **2000**, *79*, 80.
(6) Rostovtseva, T. K.; Liu, T.-T.; Colombini, M.; Parsegian, V. A.;
(7) Mafé, S.; Manzanares, J. A.; Pellicer, J. *J. Membr. Sci.* **1990**, *51*, 161.
(8) Manzanares, J. A.; Mafé, S.; Ramírez, P. *J. Non-Equilib. Thermodyn.* **1991**, *16*, 255.
(9) Peng, S.; Blachly-Dyson, E.; Forte, M.; Colombini, M.; *Biophys. J.* **1992**, *62*, 123.
(10) Zambrowicz, E. B.; Colombini, M.; *Biophys. J.* **1993**, *65*, 1093.
(11) Morrison, F. A.; Osterle, J. F. *J. Chem. Phys.* **1965**, *43*, 2111.
(12) Gross, R. J.; Osterle, J. F. *J. Chem. Phys.* **1968**, *49*, 228.
(13) Fair, J. C.; Osterle, J. F. *J. Chem. Phys.* **1971**, *54*, 3307.
(14) Westermann-Clark, G. B.; Anderson, J. L. *J. Electrochem. Soc.* **1983**, *130*, 839.
(15) Westermann-Clark, G. B.; Christoforou, C. C. *J. Electroanal. Chem.* **1986**, *198*, 213.
(16) Aguilella, V. M.; Aguilella-Arzo, M.; Ramírez, P. *J. Membr. Sci.* **1996,** *113*, 191.
(17) Aguilella, V. M.; Belaya, M.; Levadny, V. *J. Contr. Release*, **1997**, *44*, 11.
(18) The effective length of the pore is longer than the physical length because of the channel access resistance. According to the classical treatment of Hall, in practice, it means to increase the channel length by 0.8 times its diameter, hence $L = 7.5$ nm has been used for calculations. For details see refs 10 and 19.
(19) Hall, J. E. *J. Gen Physiol.* **1975**, *66*, 531.
(20) Colombini, M.; Blachly-Dyson, E.; Forte, M. In *Ion Channels*; Narahashi, T., Ed.; Plenum Publishing: New York, 1996; Vol. 4.
(21) Song, J.; Midson, C.; Blachly-Dyson, E.; Forte, M.; Colombini, M.; *Biophys. J.* **1998**, *74*, 2926.
(22) Teorell, T. *Prog. Biophys. Biophys. Chem.* **1957**, *3*, 305.
(23) Sørensen, T. S.; Koefoed, J. *J. Chem Soc., Faraday Trans. 2* **1974**, *70*, 665.